Drugs of the Future 2007, 32(10): 883-896
Copyright © 2007 PROUS SCIENCE
CCC: 0377-8282/2007
DOI: 10.1358/dof.2007.032.10.1131965

Review Article

Inhibitors of the MDM2-p53 interaction as anticancer drugs

Ian R. Hardcastle
Northern Institute for Cancer Research, Bedson Building - Chemistry, Newcastle University, NE1 7RU, U.K.

CONTENTS

Abstract

The normal functioning of the important tumor suppressor protein p53 is regulated by its binding to the MDM2 protein. Overexpression of MDM2 in some tumors is responsible for the inactivation of p53. Drugs designed to inhibit the MDM2-p53 protein-protein interaction are able to reactivate p53 activity, leading to an antitumor effect in model systems. This review details the design and discovery of small-molecule inhibitors of the MDM2-p53 interaction, which include a number of classes of potent inhibitors, such as the benzodiazepinediones, the spiro-oxindoles and the *cis*-imidazolines (nutlins). These prototype compounds have been used as experimental probes to determine the cellular consequences of activation of p53 in a variety of genetic backgrounds. The results to date indicate that small-molecule inhibitors of the MDM2-p53 interaction have great promise as antitumor agents, either as single agents or in combination with cytotoxic chemotherapy.

Introduction

The quest for novel molecular approaches to cancer therapies has bought to light many promising targets for drug discovery. Intervention at several of these molecular targets requires the identification of potent inhibitors of protein-protein interactions. In addition to the difficulties common to all drug discovery efforts, these targets face additional challenges as the interactions lack the ready-made small-molecule binding sites found in many enzymes. Good progress has been made towards inhibition of the MDM2-p53 protein-protein interaction. This review gives an overview of the target validation, structural studies and small-molecule inhibitors of MDM2-p53. To date, no MDM2-p53 inhibitors have entered clinical trials, so the increasing volume of preclinical studies of key inhibitors are detailed.

p53

The tumor suppressor protein p53 functions as a molecular node in the diverse signaling pathways resulting from cellular stresses, such as hypoxia and DNA damage. A number of kinases signal, directly and indirectly, to p53, including ATM, ATR, casein kinase I (CK I) and II (CK II), Chk1 and 2, c-Jun *N*-terminal kinase (JNK) and DNA-dependent protein kinase (DNA-PK). Phosphorylation of p53 results in the activation and stabilization of the latent tetrameric protein, which is present in low levels in normal cells, resulting in a transcriptionally active form of the protein. Activated p53 can then target a spectrum of genes responsible for a variety of cellular responses, including apoptosis and survival, *e.g.*, *APAF1*, *BAX*, *FAS*, *FDXR, IGF-BP1*, *KILLER/DR5*, *NOXA*, *PTEN* and *PUMA*, cell cycle arrest and DNA repair, *e.g., BTG2*, *CDKN1A*, *14-3-3-s*, *GADD45* and *p53R2*, angiogenesis and invasion, *e.g., TSP1*, *GD-AIF*, *BAI1*, *MMP2*, *MASPIN* and *KAI1*, and autoregulation, *e.g., MDM2*, *TP53* and *CCNG1* (1, 2). The various factors that govern the cell's decision to commit to cell cycle arrest, senescence or apoptosis have not been completely elucidated and are not yet understood. However, there is increasing evidence that the background of genetic modifications in tumor cells, *i.e.*, loss of key tumor suppressor proteins and activated oncogenic signaling, predisposes these cells to commit to the apoptotic pathway, while normal cells prefer to enter cell cycle arrest.

The loss of functional p53 is a common feature in many sporadic tumors. Mutations in the DNA-binding domain of p53 are common in around 50% of all tumors and result in the inactivation of p53-dependent pathways. Tumors expressing mutant p53 are commonly resistant to conventional chemotherapy and radiotherapy, which rely on p53-mediated responses for their effects.

MDM2

In approximately 7% of tumors and 30% of osteosarcomas and soft tissue tumors, amplification of the *MDM2* gene resulting in overexpression of the MDM2 protein is responsible for the inactivation of p53, resulting in transformation and uncontrolled tumor growth (3). The activity of p53 is tightly regulated by the MDM2 protein, which is itself transcriptionally transactivated by p53. MDM2 binds to and inactivates the p53 transactivation domain and also ubiquitylates the MDM2-p53 complex to target it for export from the nucleus and proteosomal degradation (4, 5). In normal cells, the balance between active p53 and inactive MDM2-bound p53 is maintained in a negative feedback loop (Fig. 1) (6, 7).

The importance of the correct functioning of *MDM2* in regulating *p53* was demonstrated by two *mdm2* knockout studies in mice (8, 9). The *mdm2*$^{-/-}$ mouse was found to be embryonically lethal, whereas the *p53*$^{-/-}$/*mdm2*$^{-/-}$ double knockout was viable. Interestingly, the *p53*$^{-/-}$/*mdm2*$^{-/-}$ double knockout exhibited the same phenotype as the *p53*$^{-/-}$ mouse, forming tumors within 3 months of birth (10, 11). These studies underline the principal role of *MDM2* as the master controller of *p53* activity.

Validation of the MDM2-p53 interaction as a drug target

The tractability of the MDM2-p53 interaction as a drug target was first demonstrated by the ability of short peptides to disrupt the interaction. Deletion and mutation experiments, refined by epitope mapping studies, have revealed the consensus sequences for the interaction of p53 with MDM2 (12, 13).

Preliminary experiments using phage display and synthetic peptide libraries identified the 6-mer peptide (Thr18-Phe-Ser-Asp-Leu-Trp23), corresponding to residues 18-23 of the p53 activation domain, as the consensus sequence for binding to MDM2. This peptide was able to inhibit the MDM2-p53 interaction with modest potency (IC_{50} = 700 μM). These results encouraged the search for compounds able to disrupt the MDM2-p53 interaction with greater potency, including small-molecule drug-like compounds (13).

Antisense oligodeoxyribonucleotides have revealed the consequences of the inhibition of MDM2 expression in cell lines. The *MDM2*-amplified, wild-type *p53* SJSA-1 and JAR cell lines were treated with MDM2-specific phosphorothioate oligos mediated by cationic lipids. The oligos were found to decrease the expression of MDM2, upregulate p21, activate a p53-reponsive luciferase reporter gene and induce apoptosis. Synergy with the topoisomerase I poison camptothecin was also observed (14).

The nature of the interaction between p53 and MDM2 has been determined by X-ray crystallography (15). The 109-amino-acid NH_2-terminal domain of MDM2 has been co-crystallized with an 11-amino-acid peptide fragment from the transactivation domain of p53. The X-ray structure was initially determined to 2.3 Å for *Xenopus laevis* MDM2, and then to 2.6 Å for human MDM2 by the multiple isomorphous replacement method (Fig. 2).

MDM2 forms a twisted trough around a central cleft lined with hydrophobic residues, into which the p53 peptide binds as an amphipathic α-helix. The p53 helix is orientated antiparallel to the α2 helix of MDM2 with the MDM2 middle β-sheet on the other side. Three residues (Phe19, Trp23 and Leu26) bind deep within the hydrophobic cleft, forming complementary packing interactions. The interface buries 1498 Å^2 of surface area, which is mostly hydrophobic. Two intermolecular hydrogen bonds are formed between the backbone amide of Phe19 on p53 and the Gln72 side-chain of MDM2, at the entrance of the cleft and between the p53 Trp23 indole group and the backbone carbonyl of Leu54 from MDM2, buried within the cleft.

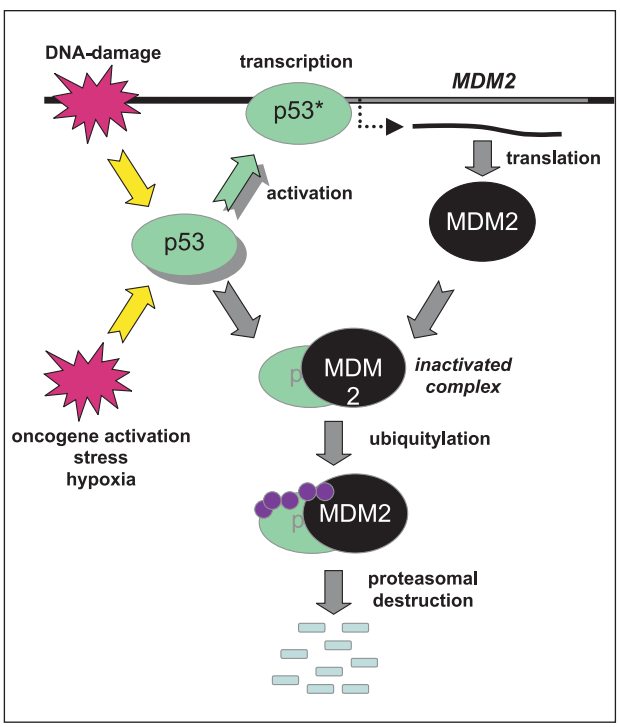

Fig. 1. The MDM2-p53 feedback loop.

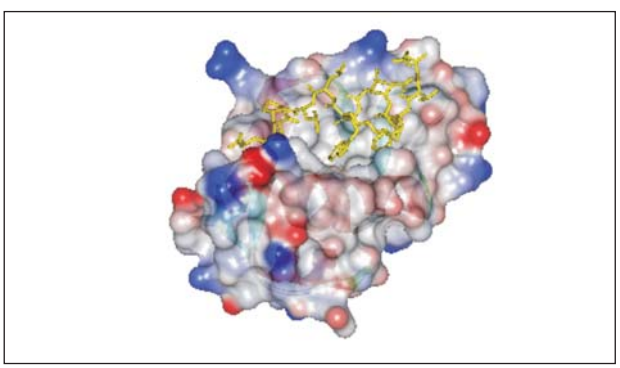

Fig. 2. X-ray structure of MDM2 bound with a p53 peptide (yellow) (pdb code: 1YCR).

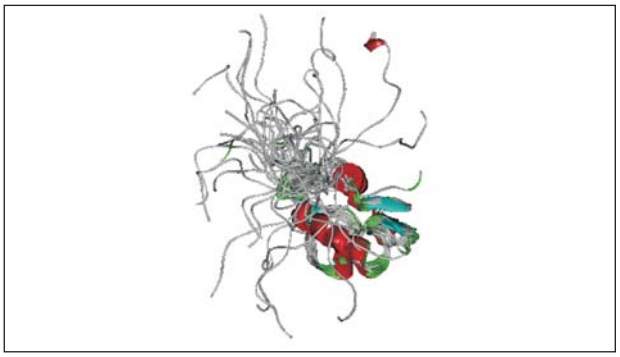

Fig. 3. NMR structure of *apo*-MDM2 (pdb code: 1Z1M).

HSQC-NMR studies have revealed that a major conformational change occurs on the binding of p53 peptides to MDM2 (16). NMR studies using *apo*-MDM2 revealed a "flexible lid" formed by residues 16-24 which appears to partly bury the p53 binding site and stabilize residues 25-109 (17). Comparison of the structure of the MDM2-p53 complex with the NMR structure of *apo*-MDM2 (1Z1M) confirms that MDM2 undergoes a number of large conformational changes upon p53 binding (Fig. 3) (18). Thus, a number of structural changes are required for the binding of p53 to MDM2: the 19-25 'lid segment' of MDM2 must vacate the p53 binding pocket; the two subdomains, comprised of β1-α1-β2-α2 and β1'-α1'-β2'-α2', must move apart by 3-4 Å, and expose the hydrophobic residues which line the pocket; and, during binding, a new β3' strand is formed as part of a (β1, β2, β3') cap at one end of the p53 binding pocket. The initiation of these events is thought to be the binding of the p53 Phe19 into the open end of the hydrophobic cleft on *apo*-MDM2. The overall conclusion from this study is that *apo*-MDM2 lacks the deep p53 binding pocket and is thus a less attractive starting point for structure-based ligand design than the MDM2 X-ray structure with p53 bound.

Inhibitors of the MDM2-p53 interaction

Peptides and peptide-derived inhibitors

The identification of the 6-mer p53 peptide, described earlier, as an MDM2-p53 inhibitor encouraged further efforts to find peptide inhibitors with greater potency. By extending the length of the peptide to 12 and 15 amino acids, inhibitors of MDM2-p53 binding with significantly greater potency than the corresponding wild-type peptide, *e.g.*, IP3 peptide (**1**; IC_{50} = 313 nM) (see Table I), were identified from phage display and synthetic peptide libraries (19). A truncated version of the lead IP3 peptide was modified to include sterically constrained α,α-disubstituted amino acids, known to stabilize α-helices, in an attempt to reduce the entropic penalties for binding to MDM2. Substitutions were made at residues which were not observed to make strong interactions with the MDM2 protein, as seen in the X-ray structure, and these resulted in the identification of peptide **3,** with 4-fold improved inhibitory activity over the corresponding peptide **2**. Further substitution of the tyrosine with a phosphonomethylphenylalanine residue (peptide **4**), designed to form a salt bridge interaction with the ε-amino group of Lys94 of MDM2, improved the affinity a further 7-fold. Finally, subsititution at the 6-position of the tyrosine residue with lipophilic groups able to fill a small cavity observed in the X-ray structure resulted in a significant increase in binding affinity. The optimal 6-substituent was chlorine, as found in the AP peptide **5** (IC_{50} = 5 nM) (20).

The cellular effects of inhibition of the MDM2-p53 interaction by peptides have been studied in a number of model systems. Expression of a GST-tagged IP3 peptide in SA1 osteosarcoma cells (*MDM2* gene-amplified, wild-type *p53*) was shown to disrupt MDM2-p53 binding, thus activating p53 and resulting in the transcription of p53, MDM2 and the p53-dependent protein $p21^{Waf1/Cip1}$. IP3 expression in SA1 cells led to inhibition of colony formation, cell cycle arrest and cell death by apoptosis (21).

The coupling of the penetratin sequence to peptides derived from the p53 amino terminal domain resulted in MDM2 antagonists with the ability to cross cell membranes (22). The effects of these compounds were investigated in a variety of rat and human cell lines. The peptides were cytotoxic to k-*ras*-transformed rat pancreatic cells (TUC-3) but not the untransformed parent cell line (BMRPA-1). Similarly, the peptides were cytotoxic to human cancer cell lines, although this effect was independent of their p53 status, indicating a p53-independent mechanism.

Despite its low cellular permeability, the AP peptide shows effects consistent with inhibition of the MDM2-p53 complex in whole cells, albeit at very high concentrations (> 100 μM). In HCT 116 cells, the AP peptide caused the accumulation of wild-type p53, $p21^{Waf1/Cip1}$ and MDM2 in a concentration-dependent manner. Similar effects were not observed in *p53*-mutant or -null cell lines. In the MDM2-overexpressing OSA-CL cell line, the AP peptide was cytotoxic, inducing apoptosis (23). Additionally the AP peptide has been coupled to the antennapedia peptide without loss of *in vitro* activity (24).

Table I: Peptide inhibitors of the MDM2-p53 interaction.

	Compound	Sequence	IC_{50} (nM)
	Wild-type p53	Ac-Gln[16]-Glu-Thr-Phe-Ser-Asp[21]-Leu-Trp-Lys-Leu-Leu-Pro[27]-NH_2	8673 ± 164
1	IP3	Ac-Met-Pro-Arg-Phe[19]-Met-Asp-Tyr-Trp-Glu-Gly-Leu[26]-Asn-NH_2	313 ± 10
2	8-mer	Ac-Phe[19]-Met-Asp-Tyr-Trp-Glu-Gly-Leu[26]-NH_2	8949 ± 85
3		Ac-Phe[19]-Met-Aib-Tyr-Trp-Glu-Ac_3c-Leu[26]-NH_2	2210 ± 346
4		Ac-Phe[19]-Met-Aib-Pmp-Trp-Glu-Ac_3c-Leu[26]-NH_2	314 ± 88
5	AP	Ac-Phe[19]-Met-Aib-Pmp-6-Cl-Trp-Glu-Ac_3c-Leu[26]-NH_2	5 ± 1

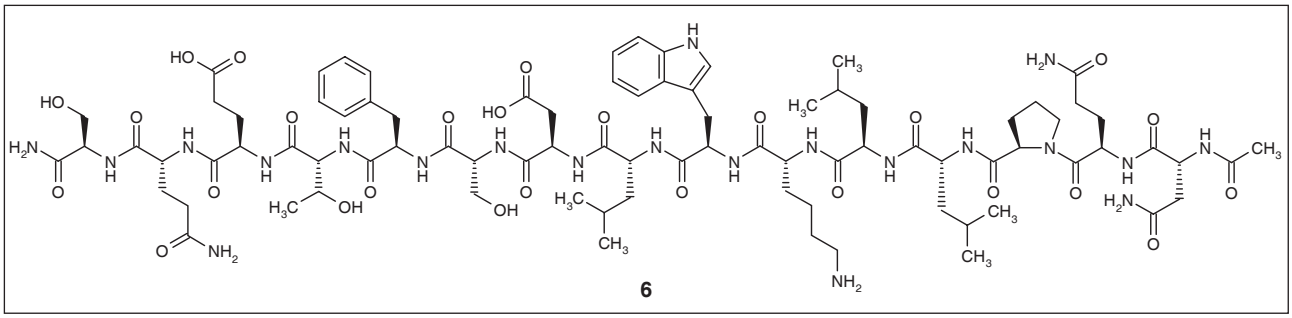

6

Retroinverso p53 peptide.

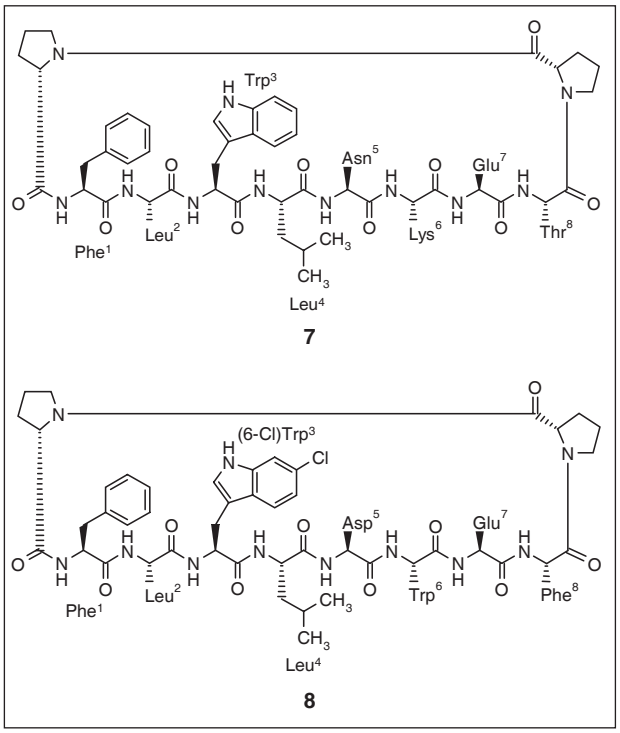

β-Hairpin peptide inhibitors.

The peptide inhibitors provide strong validation for targeting the MDM2-p53 interaction. Unlike many protein-protein interactions, the presence of a 'hot-spot' capable of binding small molecules on the target protein has been confirmed, and the cellular effects of potent inhibitors are consistent with those anticipated for inhibition of the MDM2-p53 interaction. Despite this, peptides have many serious shortcomings as potential drug molecules. A number of groups have made efforts to design more 'drug-like' molecules based on these peptides. In particular, novel methods using peptidic scaffolds designed to array the important residues in the optimal orientation for binding to MDM2 have been reported.

β-Peptides incorporate an additional backbone carbon atom, and thus are resistant to proteolysis and metabolism. A β_3-decapeptide, which formed a stable 14-helix in aqueous solution, was used as the scaffold for the p53 residues Phe19, Trp23 and Leu26 arrayed on sequential turns of the helix. Two β-peptides, β53-1 and

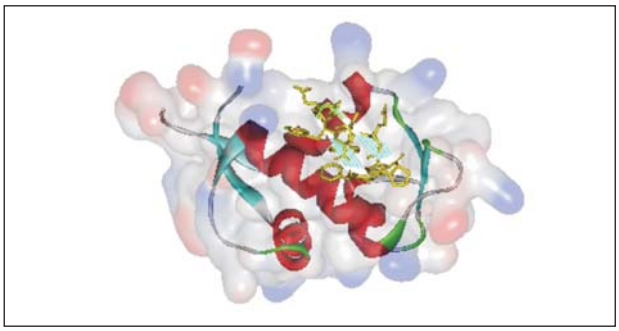

Fig. 4. X-ray structure of MDM2 bound with β-hairpin peptide **8** (pdb code: 2AXI).

β53-5, inhibited MDM2-p53 binding in a fluorescence polarization assay, albeit with modest IC_{50} values of 94.5 and 80.8 μM (25).

An unusual approach to peptide-based inhibitors of MDM2-p53 uses retroinverso peptides, *i.e.,* peptides that have the reverse sequence of amino acids to the original, which are synthesized from the unnatural D-amino acids. These D-peptides form helices with a left-handed turn, in contrast to the right-handed turn found in natural L-peptides. Despite this tendency, retroinverso peptide **6** inhibits MDM2-p53 binding with an IC_{50} of 14 μM, compared with a value of 4.2 μM for the natural 15-mer peptide (26).

The β-hairpin motif has been used as a scaffold employing a D-Pro-L-Pro dipeptide template. Computer modeling suggested that compound **7** would orientate the critical p53 residues correctly for binding to MDM2. In a BIAcore competition assay, a series of β-hairpin compounds confirmed the prediction, and the initial compound **7** displayed an IC_{50} of 125 μM. Alanine scanning demonstrated the importance of Lys6 in the binding interaction. A library of analogues was prepared incorporating variations in the MDM2-binding residues and introducing polar residues at positions 2 and 5 to improve water solubility. The Asp2, 6-Cl-Trp3 analogue (**8**) was 900-fold more potent than the parent compound (IC_{50} = 0.14 μM). The X-ray structure of **8** in complex with MDM2 has been determined (Fig. 4; PDB code 2AXI), which confirmed the β-hairpin conformation and the amphipathic nature of **8**. As predicted, the main interactions were between the hydrophobic side-chains of Phe1, (6-Cl)Trp3 and Leu4, which were buried in the p53-binding site of MDM2. Two

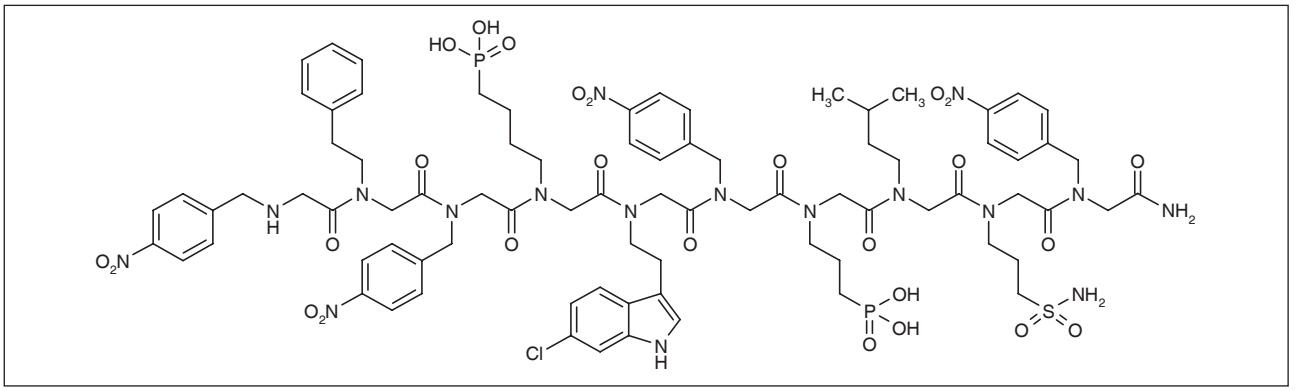

Peptoid **9**.

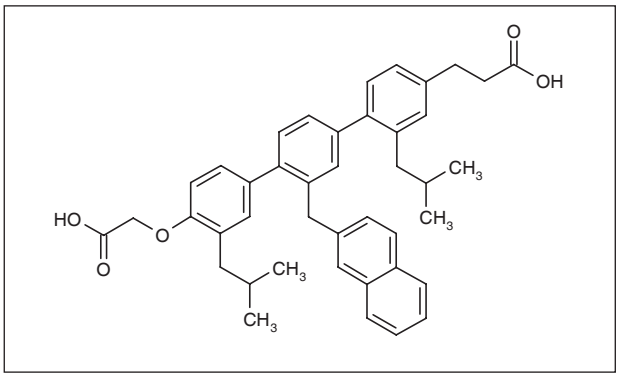

Compound **10**.

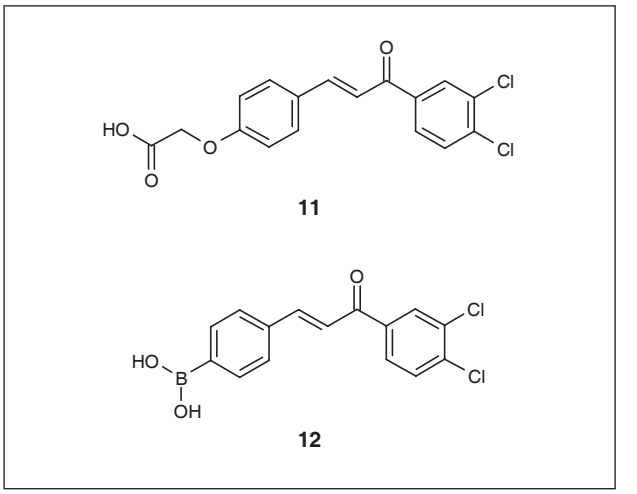

Chalcones **11** and **12.**

hydrogen bonds were seen: between (6-Cl)Trp3-NE1 and Leu54-O, and Trp6-NE1 and Lys51-NZ. Additional interactions were formed between Asp5 and surface residues of MDM2 (27, 28).

Avian pancreatic polypeptide (aPP) is a small, well-folded miniature peptide which contains an 18-residue α-helix suitable for a protein grafting approach. Key residues on this helix were varied using phage display techniques and the phage libraries panned in successive rounds against immobilized MDM2, resulting in the identification of miniature proteins optimized for MDM2 binding, with an IC_{50} range of 1.6-8.8 μM. CD spectroscopy indicated that the optimized miniature peptides had a high degree of α-helical structure necessary for high-affinity binding to MDM2 (29).

Peptoids, or oligomeric *N*-substituted glycines, have been used to make peptide-like MDM2-p53 inhibitors. The peptoid backbone has the advantage of being resistant to proteolysis and offers a wide variety of possible side-chain substituents. Importantly, the introduction of chiral side-chains can sterically bias the peptoid into forming a helical conformation. Preliminary peptoids, which incorporate the critical p53 side-chain functionality, were designed by comparison with the MDM2-p53 X-ray structure, taking into account the tighter peptoid helix. Water solubility was achieved for the peptoids by the introduction of achiral polar functional groups, such as phosphonate, sulfonamide and *p*-nitrophenyl, which could also make additional interactions with MDM2. Peptoid (**9**) showed the best inhibition of the MDM2-p53 interaction, with an IC_{50} of 6.6 μM in a fluorescence polarization assay (30).

The ability of terphenyl derivatives to mimic α-helical structures has been exploited to design MDM2-p53 inhibitors. Compound **10**, bearing two isobutyl groups and a 2-naphthylmethylene, showed good inhibition of MDM2-p53 binding, with a K_i of 0.182 μM. The binding of these terphenyl compounds to MDM2 has been studied by NMR, demonstrating that the compounds bind to the p53 binding site in a similar manner to the p53 peptide, with the 2-naphthylmethylene binding in the Trp23 binding pocket (31).

Natural product-derived inhibitors

The broad medicinal and antitumor activity observed for the chalcone class of natural products prompted their investigation as inhibitors of the MDM2-p53 interaction. Weakly active chalcones, *e.g.,* **11**, were identified using an ELISA assay and an electrophoretic band shift assay, showing release of p53 from MDM2 (32). The binding interaction of the chalcones with MDM2 was investigated

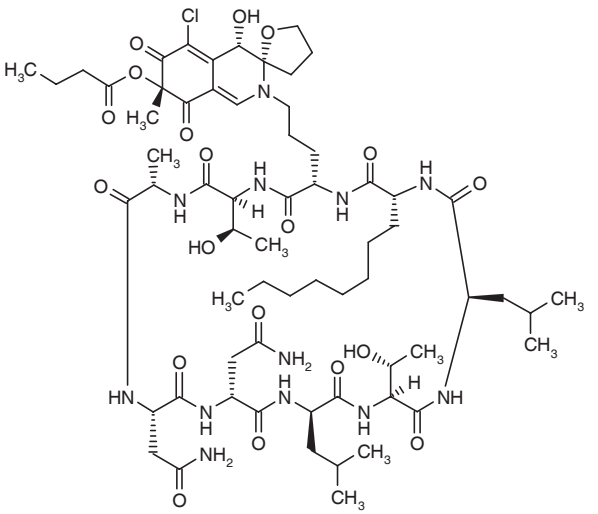

13

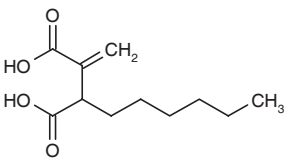

14

Natural product inhibitors chlorofusin (**13**) and (–)-hexylitaconic acid (**14**).

using 2-dimensional ^{1}H-^{15}N HSQC NMR, enabling the identification of the key ligand binding sites. The strongest interactions observed were similar to those noted for a p53-derived peptide. Further development based on these observations resulted in the identification of boronic chalcone derivatives, *e.g.,* **12**, which showed interesting activity against a panel of breast cancer cell lines (33).

A screen of over 53,000 microbial extracts generated from fermentations of a diverse collection of microorganisms identified chlorofusin (**13**) as an inhibitor of the MDM2-p53 interaction. The structure of the secondary metabolite, isolated from a strain of *Microdochium caespitosum,* was elucidated by NMR (34). Surface plasmon resonance (SPR) determinations found the K_D for binding to MDM2 to be 4.6 μM (35). Recently, (–)-hexylitaconic acid (**14**) was identified from a culture broth of *Arthrinium* sp. as an inhibitor of the MDM2-p53 interaction (IC_{50} = 50 μg/ml) (36). To date, the cellular activity of natural products **13** and **14** has not been reported.

Rational/virtual screening compounds

The publication of the X-ray structure of MDM2 bound to a p53 fragment, described earlier, enabled the application of structure-based design and virtual screening methods to the development of inhibitors of MDM2-p53 (15). A number of groups have used a variety of techniques, including docking and pharmacophore analysis, to generate models to use as the basis for virtual screening.

A series of compounds (Syc-7, -8, -11, -12 and -13) based on a 5,6-dihydroxybicyclo[2.2.1]heptane-2,3-dicarboxylic acid scaffold were designed to mimic the triad of p53 residues which bind to MDM2, based on the published X-ray crystal structure (**15**), using UNITY and DOCKING software. The five compounds shown in Figure 5 had weak inhibitory activity in an ELISA assay and showed some evidence of p53-dependent cellular activity (37).

Gatalin *et al.* used the HINT QSAR program to analyze the MDM2-p53 interaction to generate a pharmacophore model (Fig. 6), which was validated using the peptide inhibitory data (38). The pharmacophore was used as the basis of a virtual screen of the NCI 3D database. Compounds identified as hits from the screen were assayed, and the sulfonamide NSC-279287 (**15**) showed concentration-dependent inhibition, with an IC_{50} of 31.8 μM. Despite its relatively weak potency, this compound was able to induce p53-dependent transcriptional activity in SJSA-1 osteosarcoma cells stably transfected with a p53-dependent luciferase reporter gene at 1 μM (39).

Lu *et al.* used a less rigorous phamacophore, generated from the structures of MDM2 in complex with p53 peptide and several known inhibitors (Fig. 7), to generate 'hits' from a drug-like set selected from the NCI 3D database. The hits were then docked into the MDM2 structure with GOLD, using a more stringent set of parameters, and ranked using two independent scoring functions. Compounds able to bind to MDM2 mimicking the key hydrophobic interactions were screened. One compound, NSC-66811 (**16**), was identified with a K_i of 120 nM. The cellular activity of NSC-66811 was investigated in an isogenic pair of HCT 116 human colon cancer cell lines (wild-type *p53* and knockout). The compound showed strong, concentration-dependent induction of *p53*-dependent proteins in the wild-type *p53* line, but not in the *p53*-null line, over a concentration range of 0-20 μM (40).

High-throughput *in silico* screening using the LIDAEUS software (41) enabled a small-molecule database to be docked into the published X-ray structure of MDM2 (15). The approach provided the phenylthienylsulfonates **17** and phenylthienylsulfonamides **18** as hits, which was confirmed by an *in vitro* assay (42, 43).

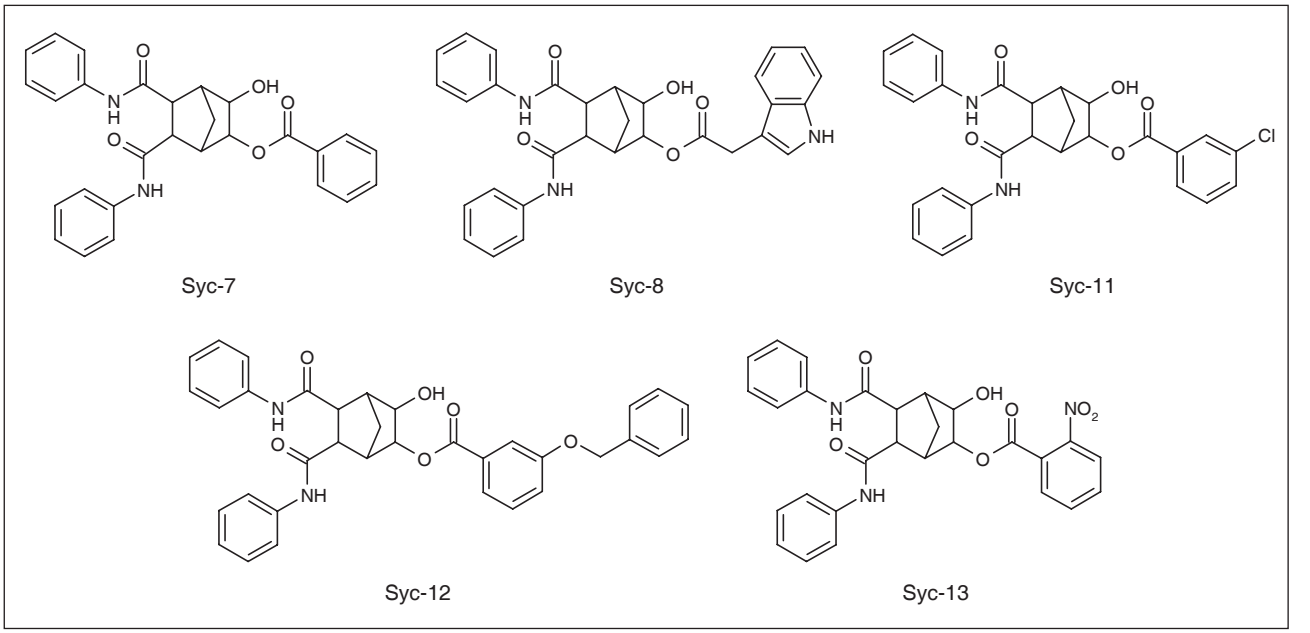

Fig. 5. Bicyclo[2.2.1]heptan-2-yl benzoate inhibitors.

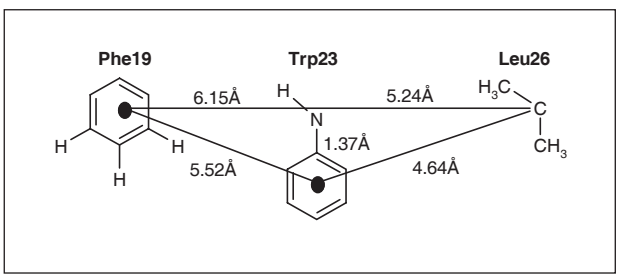

Fig. 6. QSAR pharmacophore model of the MDM2-p53 interaction (39).

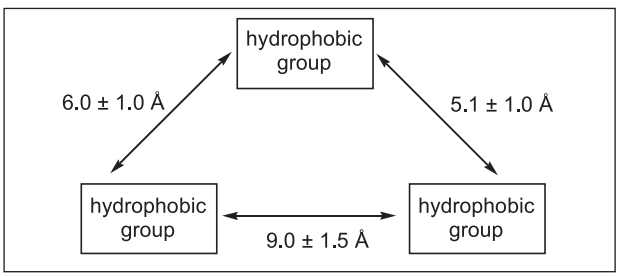

Fig. 7. Alternative pharmacophore model for MDM2-p53 inhibitors (40).

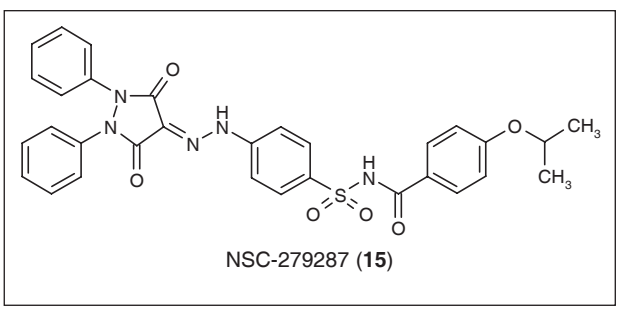

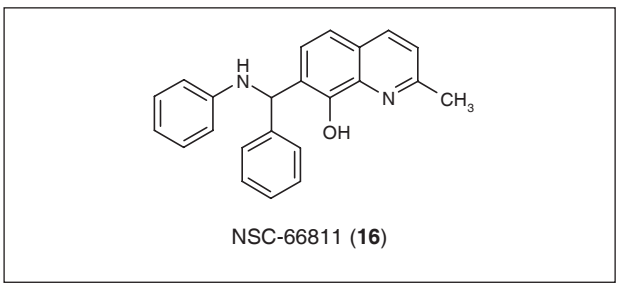

Subsequent optimization to improve potency was achieved by the addition of a 4-trifluoromethylbenzyl group onto the sulfonamide, *e.g.,* **19**. Concerns over the potential instability and reactivity of the 2-chloro-3-nitrothiophene moiety were addressed by compound **20**. The arylsulfonamides showed significant cellular activity, including induction of $p21^{Waf1/Cip1}$, induction of a p53-dependent luciferase reporter gene and induction of apoptosis in cancer cells. The compounds were not selective for wild-type *p53* cell lines, as would be expected for selective inhibitors of MDM2-p53 binding, raising the possibility that another MDM2-dependent process may also be inhibited by this class of compounds.

In silico methods have been used to develop improved inhibitors based on an isoindolinone scaffold (44). Lead compounds, with IC_{50} values ranging from 27 to 92 μM, were docked into the MDM2 structure (15) using GOLD and easyDOCK, giving a number of possible solutions for virtual screening and library synthesis. Further development resulted in the identification of isoindolinones **21** and **22** (IC_{50} = 16 and 5 μM, respectively), which showed concentration-dependent release of p53-

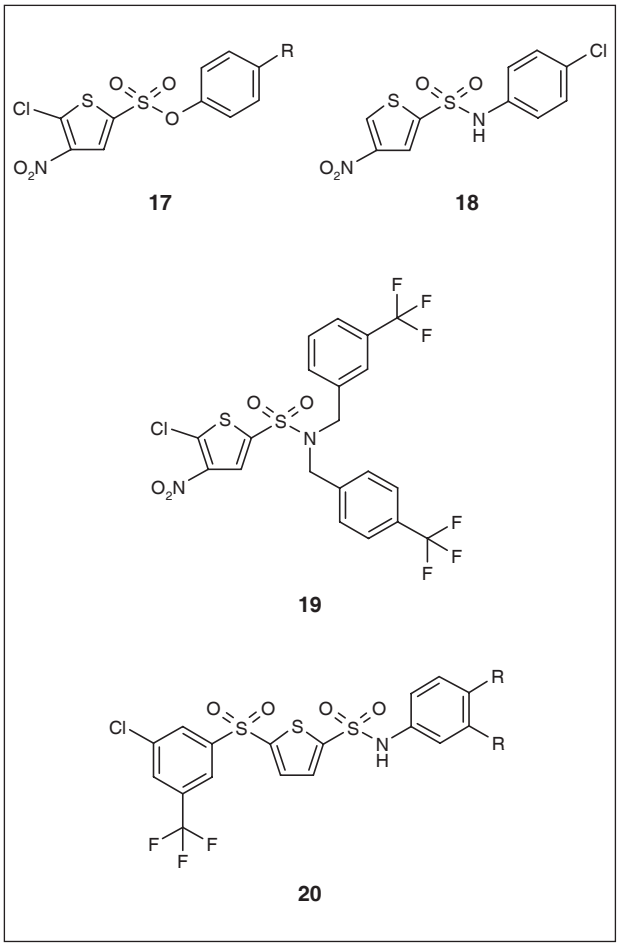

Sulfonamide inhibitors.

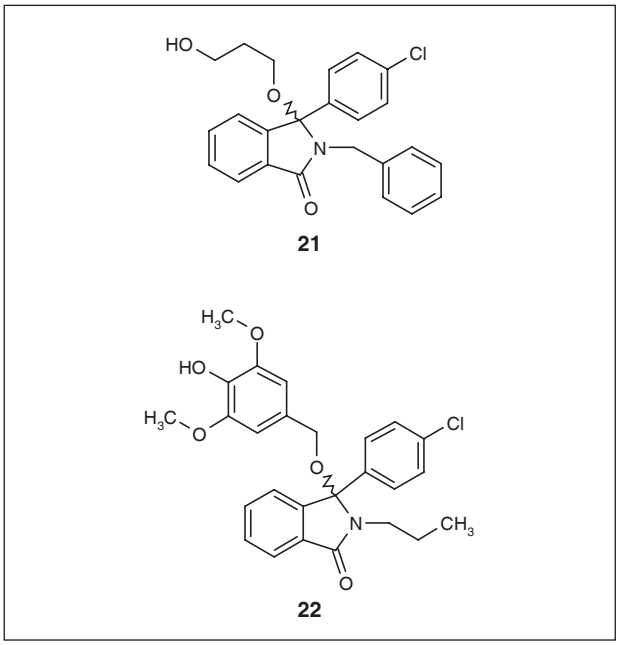

Isoindolinone inhibitors.

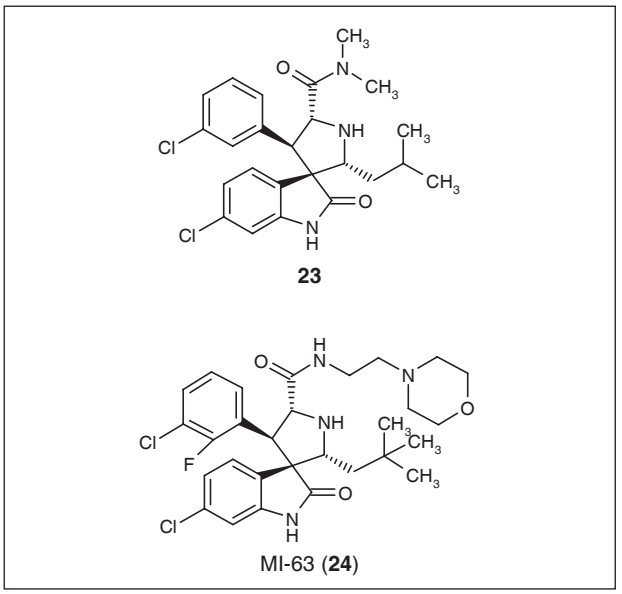

Spiro-oxindole inhibitors.

dependent transcription, resulting in increased levels of $p21^{Waf1/Cip1}$ and MDM2 in SJSA-1 cells, as probed by Western blotting, and the activation of a p53-dependent luciferase reporter gene.

A substructure search identified several natural products containing an oxindole ring, chosen as a mimic for Trp23 of p53. Modeling studies suggested that, although the natural products were unlikely to bind potently to MDM2 due to steric hinderance, the spiro(oxindole-3,3'-pyrrolidine) core structure was a promising starting point for inhibitor design (45). Subsequent design, synthesis and optimization of the series resulted in compound **23**, which has a K_i of 86 nM and inhibited the growth of the human prostate cancer cell line LNCaP with an IC_{50} value of 10.5 μM. A further round of optimization resulted in MI-63 (**24**), with a K_i of 3 nM, the most potent MDM2-p53 inhibitor disclosed to date (*c.f.,* nutlin-3 K_i = 36 nM) (46). Interestingly, the morpholino oxygen in MI-63 was found to be important for activity, and modeling suggested that it may mimic an interaction between Gln17 in p53 and Lys90 in MDM2. MI-63 caused a concentration-dependent increase in the levels of p53, MDM2 and p21 in LNCaP cells (1-5 μM) but no activation in *p53*-deleted PC-3 cells. The large induction of p53 and MDM2 observed in treated LNCaP cells prompted the authors to speculate that MI-63 was blocking the degradation of the proteins. The growth-inhibitory effects of this class of compounds showed selectivity for wild-type *p53* cells, with MI-63 showing an IC_{50} of 280 nM for LNCaP cells *versus* 18 μM for PC-3 cells, and minimal toxicity *versus* normal prostate epithelial cells at 5 μM. Excellent selectivity against other proapoptotic protein-protein targets, such as Bcl-2 and Bcl_{XL}, was also demonstrated for MI-63, which does not bind to either protein at concentrations up to 50 μM.

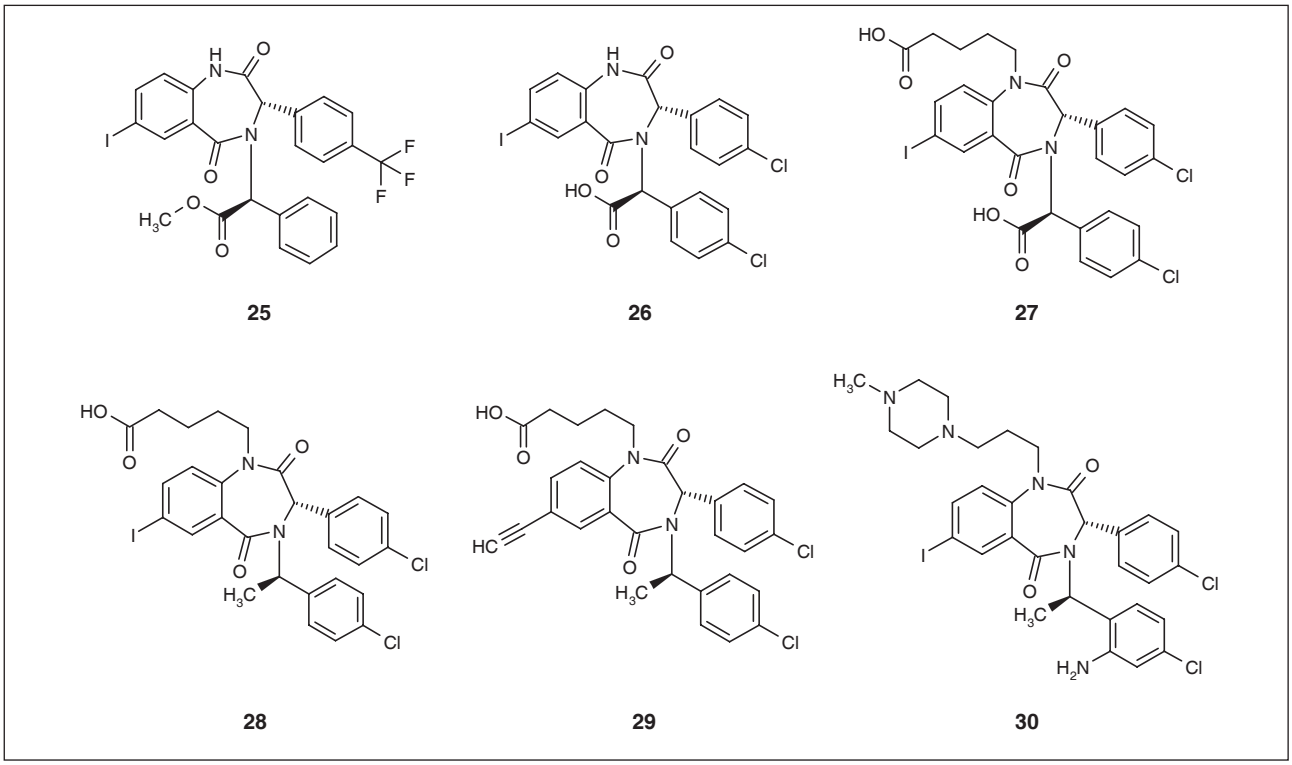

Benzodiazepinedione inhibitors.

Compounds discovered from combinatorial libraries and high-throughput screening

The screening of over 338,000 compounds from diverse combinatorial libraries for binding to MDM2 using a fluorescence-based thermal denaturation affinity assay, named ThermoFluor, resulted in the identification of a number of compounds which increased the thermal stability of the MDM2 protein (47, 48). The screening hits were characterized using a fluorescence polarization assay to determine their ability to inhibit the binding of a p53 peptide to MDM2. Hit compounds belonged to a 1,4-benzodiazepine-2,5-dione (BPD) library, *e.g.*, compound **25**. Further structural optimization showed that the carboxylic acids retained activity and gained solubility, and that the active diastereomer had the (*S*,*S*)-configuration. Replacement of the *p*-CF_3 group with *p*-Cl conferred additional potency on compound **26** (IC_{50} = 0.22 μM). The X-ray crystal structure of **26** in complex with MDM2 was determined to 2.7Å resolution, revealing that the inhibitor occupies the same space as the side-chains of Phe19, Trp23 and Leu26 of p53, making largely van der Waals interactions with the protein (Fig. 8). The poor pharmacokinetics and lack of oral bioavailability observed for **26** prompted further structural optimization (49). Modifications to the polar carboxylic acid moiety were unproductive initially. However, the introduction of a pentanoic acid group at N1 of the BDP ring (**27**, IC_{50} = 0.51 μM) was tolerated and conferred improved solubility. Re-examination of modifications at the carboxylic acid demonstrated that, with the exception of the (*R*)-methyl replacement (**28**, IC_{50} = 0.70 μM), modification resulted in a loss of potency. Structural studies suggested that the introduction of an amine group in the *ortho*-position of the chlorobenzyl moiety would be advantageous (50). The 2-anilino-4-chlorophenyl derivatives **29** and **30** bearing basic water-solubilizing groups gave the best combination of cell-free inhibition of MDM2-p53 binding (IC_{50} = 0.71 and 0.70 μM, respectively) in the fluorescence polarization assay and cellular activity as measured by the induction of the p53-inducible gene *PIG3*, and were selected for further study.

Compounds **29** and **30** both showed a differential antiproliferative effect in cell lines depending on their p53 status, and were 4- and > 10-fold more inhibitory in cells expressing wile-type *p53*, respectively (51). The ability of the compounds to disrupt the MDM2-p53 interaction in cells was demonstrated in JAR choriocarcinoma cells (*MDM2*-amplified), through immunoprecipitation with an anti-p53 antibody. Compound **29** rapidly caused a 90% dissociation of MDM2 from p53 at 40 μmol/l and was able to maintain the inhibition despite the increased MDM2 levels resulting from p53 activation. No phosphorylation of Ser15 on p53 or H2AX phosphorylation was observed in a number of cell lines, indicating that **29** does not induce DNA damage resulting in p53 stabilization. The upregulation of p53-dependent genes in HepG2 hepatocellular carcinoma cells treated with **29** was measured at the mRNA level by real-time PCR, showing a rapid induction of $p21^{waf1/cip1}$ and *MDM2*, followed by a slower induction of

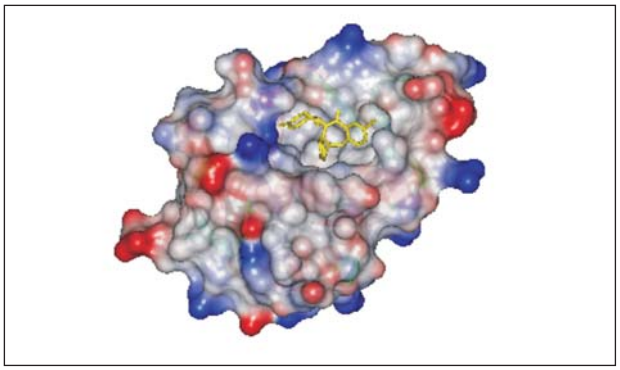

Fig. 8. X-ray structure of **26** bound to MDM2 (pdb code: 1T4E).

PIG3. These results were confirmed at the protein level by Western blotting, showing induction of PUMAα (84 times), $p21^{waf1/cip1}$ (67 times) and MDM2 (45 times). Levels of p53 increased 3-fold, probably due to the inhibition of degradation by MDM2-mediated ubiquitination. The rate of caspase-3 and -7 activation in cells treated with **29** was increased, leading to an apoptotic response. The ability of **30** to potentiate a number of chemotherapeutic agents was demonstrated in A-375 melanoma cells. Synergy was observed with doxorubicin, 5-fluorouracil and irinotecan, probably due to stabilization of p53.

Compound **30** showed better cell permeability than **29** and was therefore selected for *in vivo* studies. In a pharmacodynamic assay, mice were treated with **30** and the induction of $p21^{waf1/cip1}$ mRNA was measured by real-time PCR. A 30-fold induction was seen at the dose of 25 mg/kg, similar to that seen with the doxorubicin positive control, and a > 150-fold induction was observed at 50 mg/kg. There was no apparent toxicity with the lower dose, but weight loss was observed in the higher dose arm. The results demonstrate the *in vivo* target-based activity of **30**.

The *in vivo* efficacy of compound **30** in combination with doxorubicin was assessed in an A-375 xenograft model. Treatment with **30** alone (100 mg/kg) produced a modest effect on tumor growth, whereas the lower dose of doxorubicin alone (1.5 mg/kg) was not significantly inhibitory. The combination of **30** and doxorubicin (100 mg/kg and 1.5 mg/kg) produced a similar inhibitory effect to the higher dose of doxorubicin (3 mg/kg), but the combination was significantly less toxic than doxorubicin alone. These results suggest that small-molecule inhibitors of the MDM2-p53 interaction may have clinical utility as potentiators of cytotoxic chemotherapy.

The *cis*-imidazoline analogues **31**-**33** (nutlin-1, nutlin-2, nutlin-3), were identified through the screening of diverse synthetic libraries and named 'nutlins' (52). The compounds inhibit the MDM2-p53 interaction with IC_{50} values in the range of 100-300 nM. Separation of the enantiomers of nutlin-3 showed that one enantiomer was 150-fold more potent than the other (**33a** IC_{50} = 0.09 μM *vs*. **33b** IC_{50} = 13.6 μM). The X-ray structure of nutlin-2 in complex with MDM2 shows one bromophenyl group occupying the Trp23 pocket and the other filling the

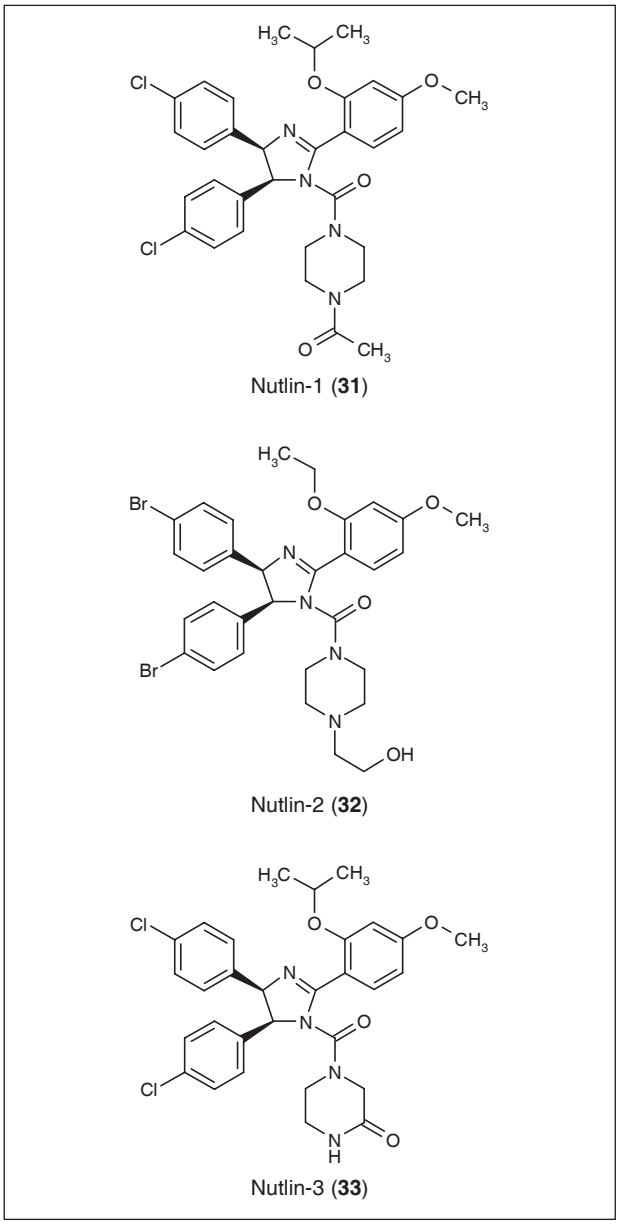

The nutlins.

Phe19 pocket (Fig. 9); the Leu26 pocket is occupied by the *ortho*-ethoxy residue, while the piperazinyl side moiety makes additional contacts with the surface of MDM2. Thus, the small *cis*-imidazoline scaffold is able to mimic an α-helical peptide in the orientation of its substituents. The structure of nutlin-1 bound to MDM2 has been determined by NMR, indicating that this analogue binds in a similar orientation to nutlin-2 (Fig. 10) (53).

Nutlin-1 displayed a concentration-dependent induction of p53, MDM2 and $p21^{waf1/cip1}$ in HCT 116 cells but not in SW480 cells (*p53*-mutant), consistent with the activation of p53. This result was confirmed by real-time PCR showing induction of $p21^{waf1/cip1}$ mRNA, while *p53* mRNA levels remained constant. Treatment with nutlin-1 did not result in p53 Ser15 phosphorylation. These results are

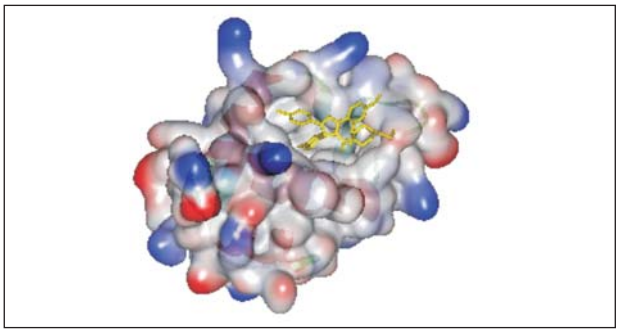

Fig. 9. X-ray structure of nutlin-2 (**32**) bound to MDM2 (pdb code:1RV1).

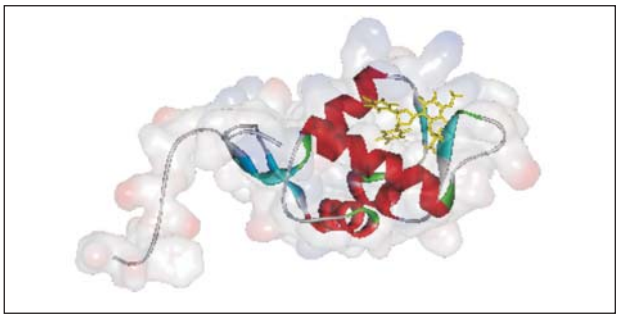

Fig. 10. NMR structure of nutlin-1 (**31**) bound to MDM2 (pdb code: 1TTV).

consistent with nutlin-1 causing activation and accumulation of p53 by post-translational stabilization. G1 and G2 cell cycle block was observed with nutlin-1 in wild-type *p53* cell lines but not in mutant *p53* cell lines. The growth-inhibitory and cytotoxic activity of nutlin-1 was also dependent on the cell line having wild-type *p53*. A similar pattern of results was observed for nutlin-3a (**33a**), but not the inactive enantiomer nutlin-3b (**33b**). Nutlin-3a induced apoptosis in SJSA-1, HCT 116 and RKO cells, whereas nutlin-3b was inactive. Interestingly, nutlin-3a inhibited the growth of human skin and mouse embryonic fibroblasts, but the cells remained viable, in contrast to the MDM2-overexpressing SJSA-1 cells which lost viability at higher concentrations. The dependence of the activity of nutlin-3a on MDM2 as a target was confirmed by the observation of the growth-inhibitory activity of the drug in mouse embyonic fibroblasts from animals with normal *p53* and *mdm2* but its inactivity in cells derived from $p53^{-/-}/mdm2^{-/-}$ double knockout mice (52, 54).

The pattern of gene expression following exposure to nutlin-3a and -3b has been compared in wild-type *p53* (HCT 116) and *p53*-null (H1299) cell lines. The active enantiomer was found to cause differential expression of 143 of 40,000 genes probed, including genes known to be associated with p53 in the wild-type *p53* cell line but not the *p53*-null line. In contrast the activity of nutlin-3b was insignificant in both cell lines (54).

The activity of nutlin-3a was investigated in a panel of 10 cell lines derived from human solid tumors, all expressing wild-type *p53*. All the cell lines examined showed induction of $p21^{waf1/cip1}$ and cell cycle arrest in the G1 and G2 phases. The apoptotic effect of the drug, as determined by flow cytometric measurement of the annexin V-positive cell fraction, was not uniform across the cell lines at 48 h. The *MDM2*-amplified SJSA-1 and MHM cell lines showed the greatest sensitivity to apoptosis, whereas the U-2 OS cell line with only one copy of the *MDM2* gene was significantly less sensitive. The gene expression profile was also compared between these cell lines and two distinct patterns were observed for the apoptosis-sensitive and -insensitive cells. The authors suggest that *MDM2* amplification is indicative of fully functioning apoptotic signaling in these cell lines, whereas the cell lines with a single *MDM2* copy may have additional defects downstream of p53 (54).

Inactivation of p53 due to overexpression of MDM2 is frequently observed in acute myeloid leukemia (AML). In AML cell lines, nutlin-3a showed a concentration-dependent antiproliferative and cytotoxic effect in two wild-type *p53* cell lines, inducing a G1/S block and accumulation of cells in the G1 phase, and apoptosis (55). These effects were not seen in the two cell lines with mutant *p53*. Samples from 18 patients with AML were also treated with nutlin-3a and the inactive enantiomer nutlin-3b. Nutlin-3a induced a concentration- and time-dependent increase in apoptotic cells in the 16 cases which expressed wild-type *p53*. There was a significant correlation between the levels of MDM2 protein and the level of apoptosis in the 16 senstitive cell lines. Interestingly, the enantiomer nutlin-3b also induced apoptosis, albeit at significantly higher concentrations.

The mechanism of nutlin-3a-induced apoptosis was also investigated in AML cell lines and wild-type *p53* cells from primary AML samples. In the cell lines, exposure to the drug resulted in a rapid induction of the p53-dependent protein Noxa, followed by caspase-9 cleavage. In the AML samples, the induction of at least one of the proapoptotic proteins Noxa, Puma and Bax was noted in each case. Apoptosis was blocked by a pan-caspase inhibitor, but not by an inhibitor of protein synthesis, suggesting that transcription-independent apoptotic pathways are also activated by nutlin-3a. The ability of nutlin-3a to synergistically potentiate the activity of the chemotherapeutic agents cytarabine and doxorubicin in AML cells at clinically relevant concentrations was also demonstrated (55).

In contrast to the synergy observed for nutlin-3a with cytarabine and doxorubicin in AML, a protective effect was observed for wild-type *p53* cancer cell lines and primary fibroblasts upon treatment with paclitaxel. The G1/S cell cycle block induced by pretreatment with nutlin-3a prevented these cells from entering the M phase. In contrast, mutant *p53* cell lines were not sensitive to the nutlins and so their sensitivity to paxlitaxel was unchanged (56).

Nutlin-3 has also been investigated in primary $CD19^{+}$ B-cell lymphocytic leukemia (B-CLL) cells. A 24-h treatment with the drug resulted in a concentration-dependent accumulation of p53 protein in both normal and leukemic cells, despite the low levels of *p53* mRNA observed in

these cells. The drug was cytotoxic to B-CLL cells, with an IC_{50} of 10.4 μM at 48 h. In contrast, an IC_{50} of > 30 μM was observed for normal B-cells, peripheral blood mononuclear cells (PBMCs), bone marrow-derived mononuclear cells (BMMCs) and $CD34^+$ hematopoietic stem cells, indicating that at concentrations lower than 10 μM nutlin-3 was tumor-selective. Nutlin-3 cytotoxicity was found to be associated with a number of apoptotic markers, *e.g.,* the presence of annexin-V, loss of $\Delta\Psi m$, loss of procaspase-3 and poly(ADP-ribose) polymerase (PARP) cleavage. Gene expression profiling revealed that a number of p53-dependent genes were upregulated at the mRNA level by nutlin-3 in B-CLL patient samples. Nutlin-3 was synergistic in combination with fludarabine in some samples (57).

The N-myc oncoprotein, important in neuroblastomas, has been shown to regulate the *MDM2* gene. The tumors normally express wild-type *p53*, and hence the effects of inhibition of the MDM2-p53 interaction with nutlin-3 and -3a has been investigated by two groups. Nutlin-3 was found to produce a concentration- and time-dependent loss of cell viability in a panel of 9 neuroblastoma cell lines with wild-type *TP53*, whereas mutant *TP53* cell lines were insensitive. Interestingly, the N-myc status of the cell lines, *i.e.*, normal or amplified, did not affect sensitivity. Cell lines sensitive to nutlin-3 showed increased mRNA levels for p53-activated genes, such as $p21^{WAF1/CIP1}$, *BAX*, *BBC3*, *PUMA* and *TP53I3,* and apoptotic markers, including DNA-laddering and caspase-3 and -7 activation. Cells that survived nutlin-3 treatment showed gross morphological changes characteristic of either senescence or neuronal differentiation, depending on the cell line and profile of gene activation. These effects were demonstrated to be p53-dependent, as they were abrogated by *p53* short hairpin RNA (shRNA) (58). Similarly, nutlin-3a was shown to induce rapid and prolonged stabilization of p53 in the IMR-32 neuroblastoma cell line, producing an apoptotic effect with an IC_{50} of 3.25 μM. Combinations of nutlin-3a and cisplatin or nutlin-3a, cisplatin and etoposide were found to be significantly more cytotoxic than cisplatin alone or in combination with etoposide (59).

Retinoblastoma cell lines have also been shown to be sensitive to nutlin-3a. WERI-Rb-1 and Y79 cell lines treated with the drug showed increased nuclear and cytoplasmic p53 levels by confocal microscopy. The drug was cytotoxic in the 5-10 μM range, and apoptosis was confirmed by annexin-V staining. The p53 dependence of nutlin-3a was demonstrated in a Y79 cell line that stably expressed *p53* small interfering RNA (siRNA). The cell line was resistant to nutlin-3a at levels consistent with the observed 70% reduction in p53 expression (60).

Nutlin-3a has been shown to radiosensitize lung cancer cell lines in a p53-dependent manner. The wild-type *p53* NCI-H460 cell line treated with nutlin-3a and ionizing radiation showed decreased survival and increased apoptosis compared to cells treated with radiation alone. In contrast, the same cell line treated with the inactive enantiomer nutlin-3b was not sensitized, and neither was the *p53*-mutant Val138 cell line (61).

The activity of nutlin-3 in cells has been demonstrated to be linked to the levels of MDMX, a homologue of MDM2. IMR-90 human lung embryonic fibroblasts transformed with E1A, RasV12 and hTERT and expressing elevated levels of MDMX were found to be resistant to nutlin-3, whereas cells with normal levels of MDMX were sensitive. Immunoprecipitation of MDM2 and MDMX showed that nutlin-3 was able to disrupt the MDM2-p53 complex, but not the complex formed with MDMX. Interestingly, MDMX-mediated resistance could be overcome by the addition of doxorubicin, as MDMX-p53 complexes are disrupted by phosphorylation in response to DNA damage (62, 63).

The *in vivo* efficacy of nutlin-3 was determined in an SJSA-1 osteosarcoma xenograft when dosed at 200 mg/kg twice daily for 20 days, resulting in 90% inhibition of tumor growth, with no toxicity or weight loss. The authors commented that the activation of p53 in xenografts affected growth by a number of mechanisms, including effects on the tumor microenvironment (62). Additional experiments using the active nutlin-3a enantiomer have confirmed the activity of the drug in the SJSA-1 xenograft model, with 8 partial and 1 full regressions after dosing with 200 mg/kg twice daily for 3 weeks. Similar effects were seen for MHM, LNCaP and 22Rv1 cells, with *mdm2*-amplified MHM tumors showing similar sensitivity to SJSA-1 tumors. The authors conclude that therapy with MDM2 antagonists is most promising for *MDM2*-amplified tumors, and that other tumors with functioning p53-activated apoptotic pathways would also be likely to respond (54).

Conclusions

A detailed understanding of the role of MDM2 in the regulation of p53 activity has identified the MDM2-p53 protein-protein interaction as a rational target for drug discovery. The nature of the interaction, through the binding of a p53 α-helix into a complementary cleft on MDM2, makes it a promising target for small-molecule therapeutics. A number of chemical classes of MDM2-p53 inhibitors have been discovered using rational design and screening approaches. The most potent and drug-like compounds, *e.g.,* the benzodiazepinediones, the spiro-oxindoles and the *cis*-imidazolines (nutlins), show potent cellular activation of p53-dependent transcription. The biological consequences of p53 activation are dependent on the genetic background of the treated cells, with sensescence or apoptosis resulting in many tumor cell lines. Preliminary *in vivo* experiments indicate selective antitumor effect either as single agents or in combination with cytotoxic chemotherapy. Despite the promising results published to date, MDM2-p53 inhibitors have not yet entered clinical trials. The apparent delay in development may be due to both the novelty of protein-protein antagonists as drugs and the complexity of the biological target. In the meantime, potent inhibitors such as nutlin-3 are being used to elucidate p53 signaling pathways and identify the tumor types most likely to respond to this therapeutic approach.

References

1. Lane, D.P. *Cancer. p53, guardian of the genome.* Nature 1992, 358: 15-6.

2. Vousden, K.H., Lu, X. *Live or let die: The cell's response to p53.* Nat Rev Cancer 2002, 2: 594-604.

3. Oliner, J.D., Kinzler, K.W., Meltzer, P.S., George, D.L., Vogelstein, B. *Amplification of a gene encoding a p53-associated protein in human sarcomas.* Nature 1992, 358: 80-3.

4. Haupt, Y., Maya, R., Kazaz, A., Oren, M. *Mdm2 promotes the rapid degradation of p53*. Nature 1997, 387: 296-9.

5. Kubbutat, M.H.G., Jones, S.N., Vousden, K.H. *Regulation of p53 stability by Mdm2.* Nature 1997, 387: 299-303.

6. Momand, J., Zambetti, G.P., Olson, D.C., George, D., Levine, A. *The mdm-2 oncogene product forms a complex with p53 protein and inhibits p53-mediated transactivation*. Cell 1992, 69: 1237-45.

7. Fuchs, S.Y., Adler, V., Buschmann, T., Wu, X.W., Ronai, Z. *Mdm2 association with p53 targets its ubiquitination.* Oncogene 1998, 17: 2543-7.

8. Jones, S.N., Roe, A.E., Donehower, L.A., Bradley, A. *Rescue of embryonic lethality in Mdm2-deficient mice by absence of p53.* Nature 1995, 378: 206-8.

9. de Oca Luna, R.M., Wagner, D.S., Lozano, G. *Rescue of early embryonic lethality in mdm2-deficient mice by deletion of p53*. Nature 1995, 378: 203-6.

10. Donehower, L.A., Harvey, M., Slagle, B.L., McArthur, M.J., Montgomery, C.A., Butel, J.S., Allan, B. *Mice deficient for p53 are developmentally normal but susceptible to spontaneous tumours.* Nature 1992, 356: 215-21.

11. Jones, S.N., Sands, A.T., Hancock, A.R. et al. *The tumorigenic potential and cell growth characteristics of p53-deficient cells are equivalent in the presence or absence of Mdm2.* Proc Natl Acad Sci USA 1996, 93: 14106-11.

12. Oliner, J.D., Pietenpol, J.A., Thiagalingam, S., Gvuris, J., Kinzler, K.W., Vogelstein, B. *Oncoprotein Mdm2 conceals the activation domain of tumor suppressor-p53*. Nature 1993, 362: 857-60.

13. Picksley, S.M., Vojtesek, B., Sparks, A., Lane, D.P. *Immunochemical analysis of the interaction of p53 with MDM2; - Fine mapping of the MDM2 binding site on p53 using synthetic peptides.* Oncogene 1994, 9: 2523-9.

14. Chen, L., Agrawal, S., Zhou, W., Zhang, R., Chen, J. *Synergistic activation of p53 by inhibition of MDM2 expression and DNA damage.* Proc Natl Acad Sci USA 1998, 95: 195-200.

15. Kussie, P.H., Gorina, S., Marechal, V., Elenbaas, B., Moreau, J., Levine, A.J., Pavletich, N.P. *Structure of the MDM2 oncoprotein bound to the p53 tumor suppressor transactivation domain.* Science 1996, 274: 948-53.

16. Schon, O., Friedler, A., Bycroft, M., Freund, S.M.V., Fersht, A.R. *Molecular mechanism of the interaction between MDM2 and p53.* J Mol Biol 2002, 323: 491-501.

17. McCoy, M.A., Gesell, J.J., Senior, M.M., Wyss, D.F. *Flexible lid to the p53-binding domain of human Mdm2: Implications for p53 regulation.* Proc Natl Acad Sci USA 2003, 100: 1645-8.

18. Uhrinova, S., Uhrin, D., Powers, H. et al. *Structure of free MDM2 N-terminal domain reveals conformational adjustments that accompany p53-binding.* J Mol Biol 2005, 350: 587-98.

19. Bottger, V., Bottger, A., Howard, S.F. et al. *Identification of novel mdm2 binding peptides by phage display.* Oncogene 1996, 13: 2141-7.

20. Garcia-Echeverria, C., Chene, P., Blommers, M.J.J., Furet, P. *Discovery of potent antagonists of the interaction between human double minute 2 and tumor suppressor p53*. J Med Chem 2000, 43: 3205-8.

21. Wasylyk, C., Salvi, R., Argentini, M. et al. *p53 mediated death of cells overexpressing MDM2 by an inhibitor of MDM2 interaction with p53.* Oncogene 1999, 18: 1921-34.

22. Kanovsky, M., Raffo, A., Drew, L. et al. *Peptides from the amino terminal mdm-2-binding domain of p53, designed from conformational analysis, are selectively cytotoxic to transformed cells.* Proc Natl Acad Sci USA 2001, 98: 12438-43.

23. Chene, P., Fuchs, J., Bohn, J., Garcia-Echeverria, C., Furet, P., Fabbro, D. *A small synthetic peptide, which inhibits the p53-hdm2 interaction, stimulates the p53 pathway in tumour cell lines.* J Mol Biol 2000, 299: 245-53.

24. Garcia-Echeverria, C., Furet, P., Chene, P. *Coupling of the antennapedia third helix to a potent antagonist of the p53/hdm2 protein-protein interaction.* Bioorg Med Chem Lett 2001, 11: 2161-4.

25. Kritzer, J.A., Lear, J.D., Hodsdon, M.E., Schepartz, A. *Helical beta-peptide inhibitors of the p53-hDM2 interaction.* J Am Chem Soc 2004, 126: 9468-9.

26. Sakurai, K., Chung, H.S., Kahne, D. *Use of a retroinverso p53 peptide as an inhibitor of MDM2.* J Am Chem Soc 2004, 126: 16288-9.

27. Fasan, R., Dias, R.L.A., Moehle, K., Zerbe, O., Vrijbloed, J.W., Obrecht, D., Robinson, J.A. *Using a β-hairpin to mimic an α-helix: Cyclic peptidomimetic inhibitors of the p53-HDM2 protein-protein interaction.* Angewandte Chem Int Ed 2004, 43: 2109-12.

28. Fasan, R., Dias, R.L.A., Moehle, K.A. et al. *Structure-activity studies in a family of β-hairpin protein epitope mimetic inhibitors of the p53-HDM2 protein-protein interaction.* ChemBioChem 2006, 7: 515-26.

29. Kritzer, J.A., Zutshi, R., Cheah, M., Ran, F.A., Webman, R., Wongjirad, T.M., Schepartz, A. *Miniature protein inhibitors of the p53-hDM2 interaction*. ChemBioChem 2006, 7: 29-31.

30. Hara, T., Durell, S.R., Myers, M.C., Appella, D.H. *Probing the structural requirements of peptoids that inhibit HDM2-p53 interactions.* J Am Chem Soc 2006, 128: 1995-2004.

31. Yin, H., Lee, G.I., Park, H.S., Payne, G.A., Rodriguez, J.M., Sebti, S.M., Hamilton, A.D. *Terphenyl-based helical mimetics that disrupt the p53/HDM2 interaction.* Angewandte Chem Int Ed 2005, 44: 2704-7.

32. Stoll, R., Renner, C., Hansen, S. et al. *Chalcone derivatives antagonize interactions between the human oncoprotein MDM2 and p53.* Biochemistry 2001, 40: 336-44.

33. Kumar, S.K., Hager, E., Pettit, C., Gurulingappa, H., Davidson, N.E., Khan, S.R. *Design, synthesis, and evaluation of novel boronic-chalcone derivatives as antitumor agents.* J Med Chem 2003, 46: 2813-5.

34. Duncan, S.J., Gruschow, S., Williams, D.H. et al. *Isolation and structure elucidation of chlorofusin, a novel p53-MDM2 antagonist from a Fusarium sp.* J Am Chem Soc 2001, 123: 554-60.

35. Duncan, S.J., Cooper, M.A., Williams, D.H. *Binding of an inhibitor of the p53/MDM2 Interaction to MDM2.* Chem Commun 2003, 316-7.

36. Tsukamoto, S., Yoshida, T., Hosono, H., Ohta, T., Yokosawa, H. *Hexylitaconic acid: A new inhibitor of p53-HDM2 interaction isolated from a marine-derived fungus, Arthrinium sp.* Bioorg Med Chem Lett 2006, 16: 69-71.

37. Zhao, J.H., Wang, M.J., Chen, J. et al. *The initial evaluation of non-peptidic small-molecule HDM2 inhibitors based on p53-HDM2 complex structure.* Cancer Lett 2002, 183: 69-77.

38. Galatin, P.S., Abraham, D.J. *QSAR: Hydropathic analysis of inhibitors of the p53-mdm2 interaction.* Prot Struct Funct Genet 2001, 45: 169-75.

39. Galatin, P.S., Abraham, D.J. *A nonpeptidic sulfonamide inhibits the p53-mdm2 interaction and activates p53-dependent transcription in mdm2-overexpressing cells.* J Med Chem 2004, 47: 4163-5.

40. Lu, Y., Nikolovska-Coleska, Z., Fang, X. et al. *Discovery of a nanomolar inhibitor of the human murine double minute 2 (MDM2)-p53 interaction through an integrated, virtual database screening strategy.* J Med Chem 2006, 49: 3759-62.

41. Wu, S.Y., McNae, I., Kontopidis, G. et al. *Discovery of a novel family of CDK inhibitors with the program LIDAEUS: Structural basis for ligand-induced disordering of the activation loop.* Structure 2003, 11: 399-410.

42. Zheleva, D.I., McInnes, C., Baxter, C. et al. *Bisarylsulfonamides - Novel small molecule inhibitors of p53-Mdm2 interaction.* Proc Am Assoc Cancer Res (AACR) 2004, 45: Abst 5552.

43. Fischer, P. *Peptide, peptidomimetic, and small-molecule antagonists of the p53-HDM2 protein-protein interaction.* Int J Pept Res Ther 2006, 12: 3-19.

44. Hardcastle, I.R., Ahmed, S.U., Atkins, H. et al. *Isoindolinone based inhibitors of the MDM2-p53 protein-protein interaction.* Bioorg Med Chem Lett 2005, 15: 1515-20.

45. Ding, K., Lu, Y., Nikolovska-Coleska, Z. et al. *Structure-based design of potent non-peptide MDM2 inhibitors.* J Am Chem Soc 2005, 127: 10130-1.

46. Ding, K., Lu, Y., Nikolovska-Coleska, Z. et al. *Structure-based design of spiro-oxindoles as potent, specific small-molecule inhibitors of the MDM2-p53 interaction.* J Med Chem 2006, 49: 3432-5.

47. Parks, D.J., LaFrance, L.V., Calvo, R.R. et al. *1,4-Benzodiazepine-2,5-diones as small molecule antagonists of the HDM2-p53 interaction: Discovery and SAR.* Bioorg Med Chem Lett 2005, 15: 765-70.

48. Grasberger, B.L., Lu, T.B., Schubert, C. et al. *Discovery and cocrystal structure of benzodiazepinedione HDM2 antagonists that activate p53 in cells.* J Med Chem 2005, 48: 909-12.

49. Parks, D.J., LaFrance, L.V., Calvo, R.R. et al. *Enhanced pharmacokinetic properties of 1,4-benzodiazepine-2,5-dione antagonists of the HDM2-p53 protein-protein interaction through structure-based drug design.* Bioorg Med Chem Lett 2006, 16: 3310-4.

50. Marugan, J.J., Leonard, K., Raboisson, P. et al. *Enantiomerically pure 1,4-benzodiazepine-2,5-diones as Hdm2 antagonists.* Bioorg Med Chem Lett 2006, 16: 3115-20.

51. Koblish, H.K., Zhao, S.Y., Franks, C.F. et al. *Benzodiazepinedione inhibitors of the Hdm2:p53 complex suppress human tumor cell proliferation in vitro and sensitize tumors to doxorubicin in vivo.* Mol Cancer Ther 2006, 5: 160-9.

52. Vassilev, L.T., Vu, B.T., Graves, B. et al. *In vivo activation of the p53 pathway by small-molecule antagonists of MDM2.* Science 2004, 303: 844-8.

53. Fry, D.C., Emerson, S.D., Palmeb, S., Vua, B.T., Liua, C.-M., Podlaskia, F. *NMR structure of a complex between MDM2 and a small molecule inhibitor.* J Biomol NMR 2004, 30: 163-73.

54. Tovar, C., Rosinski, J., Filipovic, Z. et al. *Small-molecule MDM2 antagonists reveal aberrant p53 signaling in cancer: Implications for therapy.* Proc Natl Acad Sci USA 2006, 103: 1888-93.

55. Kojima, K., Konopleva, M., Samudio, I.J. et al. *MDM2 antagonists induce p53-dependent apoptosis in AML: Implications for leukemia therapy.* Blood 2005, 106: 3150-9.

56. Carvajal, D., Tovar, C., Yang, H., Vu, B.T., Heimbrook, D.C., Vassilev, L.T. *Activation of p53 by MDM2 antagonists can protect proliferating cells from mitotic inhibitors.* Cancer Res 2005, 65: 1918-24.

57. Secchiero, P., Barbarotto, E., Tiribelli, M. et al. *Functional integrity of the p53-mediated apoptotic pathway induced by the nongenotoxic agent nutlin-3 in B-cell chronic lymphocytic leukemia (B-CLL).* Blood 2006, 107: 4122-9.

58. Van Maerken, T., Speleman, F., Vermeulen, J. et al. *Small-molecule MDM2 antagonists as a new therapy concept for neuroblastoma.* Cancer Res 2006, 66: 9646-55.

59. Barbieri, E., Mehta, P., Chen, Z., Zhang, L., Slack, A., Berg, S., Shohet, J.M. *MDM2 inhibition sensitizes neuroblastoma to chemotherapy-induced apoptotic cell death.* Mol Cancer Ther 2006, 5: 2358-65.

60. Elison, J.R., Cobrinik, D., Claros, N., Abramson, D.H., Lee, T.C. *Small molecule inhibition of HDM2 leads to p53-mediated dell death in retinoblastoma cells.* Arch Ophthalmol 2006, 124: 1269-75.

61. Cao, C., Shinohara, E.T., Subhawong, T.K. et al. *Radiosensitization of lung cancer by nutlin, an inhibitor of murine double minute 2.* Mol Cancer Ther 2006, 5: 411-7.

62. Patton, J.T., Mayo, L.D., Singhi, A.D., Gudkov, A.V., Stark, G.R., Jackson, M.W. *Levels of HdmX expression dictate the sensitivity of normal and transformed cells to nutlin-3.* Cancer Res 2006, 66: 3169-76.

63. Hu, B., Gilkes, D.M., Farooqi, B., Sebti, S.M., Chen, J. *MDMX overexpression prevents p53 activation by the MDM2 inhibitor nutlin.* J Biol Chem 2006, 281: 33030-5.